

Strength and Trans Influence of the Rh–Rh Bond in Rhodium(II) Carboxylate Dimers

Joe G. Norman, Jr.,* and Harold J. Kolari

Contribution from the Department of Chemistry, University of Washington, Seattle, Washington 98195. Received July 18, 1977

Abstract: SCF– $X\alpha$ –SW calculations of $\text{Rh}_2(\text{O}_2\text{CH})_4(\text{H}_2\text{O})_2$ and $\text{Rh}_2(\text{O}_2\text{CH})_4$ are used to discuss the electronic structures of rhodium(II) carboxylates, $\text{Rh}_2(\text{CO}_3)_4^{4-}$, $\text{Rh}_2(\text{SO}_4)_4^{4-}$, and $\text{Rh}_2^{4+}(\text{aq})$. The Rh–Rh bonds in these compounds are predicted to be single, not triple; the basic orbital configuration is $\sigma^2\pi^4\delta^2\pi^*4\delta^*2$. Reasons for the short Rh–Rh distance of 2.39 Å in $\text{Rh}_2(\text{O}_2\text{CCH}_3)_4(\text{H}_2\text{O})_2$ are discussed in this context. Both a detailed description and a simple orbital picture of how the Rh–Rh bond so dramatically weakens the trans Rh–OH₂ bonds are given; the key is the Rh–OH₂ antibonding character of Rh–Rh σ and σ^* orbitals. The converse effect of axial ligands on the Rh–Rh bond is also discussed. Comparisons are made with previous calculations on quadruply bonded complexes, particularly $\text{Mo}_2(\text{O}_2\text{CH})_4$. The peaks at 17.1, 22.7, 40 sh, and $45.9 \times 10^{-3} \text{ cm}^{-1}$ in the electronic spectrum of $\text{Rh}_2(\text{O}_2\text{CCH}_3)_4(\text{H}_2\text{O})_2$ are assigned to $\pi^* \rightarrow \sigma^*$, $\pi^* \rightarrow \text{Rh–O } \sigma^*$, $\sigma \rightarrow \sigma^*$, and $L\sigma \rightarrow \sigma^*$ transitions, respectively. The recently isolated diatomic Rh_2 is predicted to have an $S = 2$ ground state at Rh–Rh = 2.39 Å, based on a “ $d^{17}s^1$ ” configuration; comparisons are made to Mo_2 . The ground state of $[\text{Ru}_2(\text{O}_2\text{CR})_4]^+$ compounds is predicted to be $\sigma^2\pi^4\delta^2\pi^*2\delta^*1$.

We have previously analyzed the quadruple metal–metal bonds¹ in $\text{Mo}_2\text{Cl}_8^{4-}$ and $\text{Mo}_2(\text{O}_2\text{CH})_4$, and their interactions with metal–ligand bonds, using SCF– $X\alpha$ –SW calculations.^{2,3} Others have reported similar calculations on $\text{Re}_2\text{Cl}_8^{2-}$ ⁴ and $\text{Cr}_2(\text{O}_2\text{CH})_4$;⁵ SCF–HF–LCAO treatments of d^4 – d^4 dimers are also beginning to appear.^{6,7} The combination of the $X\alpha$ –SW calculations and careful experimental investigations of electronic,^{4,8–12} photoelectron,^{6,13,14} resonance Raman,^{11,15} and EPR¹⁶ spectra have greatly increased understanding of the electronic structures of these important compounds.

The dinuclear M_2L_8 structure of D_{4h} symmetry common to nearly all the d^4 – d^4 dimers is also known for a smaller number of compounds where the metals have other d^n configurations.¹ Prominent among these are the carboxylates $M_2(\text{O}_2\text{CR})_4L_2$ ($L =$ axial ligand), which have been structurally characterized not only for Cr(II), Mo(II), and Re(III), but also for Ru(2.5),¹⁷ Co(II),¹⁸ Rh(II),¹⁹ and Cu(II).²⁰ Just as considerable controversy has surrounded the assignment of electronic spectra for the d^4 – d^4 dimers, so there has been much discussion of what the metal–metal bond orders are in these latter compounds containing d^5 , d^7 , and d^9 metals. Indeed the question is the same in both cases: what is the nature and ordering of the orbitals having higher energy than the metal–metal σ , π , and δ bonding levels (which are just filled in the d^4 – d^4 systems)? The calculations and experiments mentioned above were largely stimulated by, and have essentially settled, this question for the quadruply bonded molecules. We are presently carrying out $X\alpha$ –SW calculations on Ru(2.5), Rh(II), and Cu(II) carboxylate dimers in hopes of achieving a similar resolution for these systems.

The background of opposing views about the Rh(II) case is as follows. The initial report of the crystal structure of $\text{Rh}_2(\text{O}_2\text{CCH}_3)_4(\text{H}_2\text{O})_2$ contained the proposal that a Rh–Rh single bond was present.²¹ A later extended–Hückel calculation supported this view, giving the electronic configuration $\sigma^2\pi^4\delta^2\pi^*2\pi^*4$, and allowing a consistent interpretation of observed variations in the electronic spectrum upon changing the axial ligands from H_2O to stronger donors.²² In the meantime, however, Cotton had pointed out that the short Rh–Rh distance, now accurately known as 2.386 (1) Å,¹⁹ was more consistent with a multiple interaction.^{19,23} Rh–Rh bonds which are unambiguously single usually have lengths of 2.7–2.8 Å;^{1,24} estimates in this range are also obtained using Rh covalent radii derived from metal–ligand distances.^{19,25} In particular, he suggested a triple bond, based on the electronic configuration $\sigma^2\pi^4\delta^2\sigma_n^2\sigma_n'^2\delta^*2$. The σ_n and σ_n' orbitals are essentially non-

bonding d_{z^2} hybrids directed outward from the ends of the metal–metal axis. Although the recent theoretical and experimental work on the d^4 – d^4 systems shows these orbitals to be nonexistent in the appropriate energy range, it is not clear whether the same orbital diagram would apply to a d^7 – d^7 case.²⁶

In this paper we offer conclusions, based on an SCF– $X\alpha$ –SW treatment of $\text{Rh}_2(\text{O}_2\text{CH})_4(\text{H}_2\text{O})_2$, which we believe go far toward settling this longstanding controversy. Our results should also apply to the complexes $\text{Rh}_2(\text{CO}_3)_4^{4-}$, $\text{Rh}_2(\text{SO}_4)_4^{4-}$, and $\text{Rh}_2(\text{H}_2\text{O})_{10}^{4+}$, whose spectra indicate entirely analogous electronic structures to the carboxylates.²⁷ We also consider the general phenomenon of the metal–metal trans influence²⁸ by comparing calculations on $\text{Rh}_2(\text{O}_2\text{CH})_4(\text{H}_2\text{O})_2$ and $\text{Rh}_2(\text{O}_2\text{CH})_4$. A large number of experimental observations have established that certain ligands produce abnormally weak bonds to metals for other ligands bound trans to them.^{29–31} The data suggest that the most influential ligands in this respect are those which form strong, covalent σ bonds to the metal.³² On this basis, one would expect other metals to be among the strongest trans-influencing ligands. The structures of the dinuclear carboxylates, some of which are summarized in Table I, confirm this hypothesis. As the metal–metal bond strengthens, the metal–axial ligand bond weakens, becoming 0.4–0.6 Å longer than normal when the trans metal is quadruply bonded. Our calculations reveal quantitative details of this phenomenon which translate into a simple qualitative understanding. Finally, we discuss in a preliminary manner the electronic structures of the recently isolated diatomic molecule Rh_2^{34} and Ru(2.5) carboxylate dimers.

Computational Section

Atomic coordinates for the calculations of $\text{Rh}_2(\text{O}_2\text{CH})_4(\text{H}_2\text{O})_2$, $\text{Rh}_2(\text{O}_2\text{CH})_4$, and Rh_2 were all based on the x-ray structure of $\text{Rh}_2(\text{O}_2\text{CCH}_3)_4(\text{H}_2\text{O})_2$.¹⁹ Specifically, the bond parameters used were Rh–Rh = 2.39 Å, Rh–O₂CH = 2.04 Å, Rh–OH₂ = 2.31 Å, C–O = 1.27 Å, C–H = 1.08 Å, O–H = 0.99 Å, angle O–C–O = 125°, and angle H–O–H = 120°. The coordinate systems for $\text{Rh}_2(\text{O}_2\text{CH})_4$ (D_{4h} symmetry) and $\text{Rh}_2(\text{O}_2\text{CH})_4(\text{H}_2\text{O})_2$ (D_{2h} symmetry) are shown below by a perspective drawing and a z-axis projection, respectively.

Overlapping atomic sphere radii were obtained by our nonempirical procedure³⁵ and are given in Table II. They represent 91.0, 89.3, and 85.0% of the atomic-number radii for

Table I. Bond Lengths (Å) in Some $M_2(O_2CR)_4L_2$ Compounds (L = Axial Ligand)

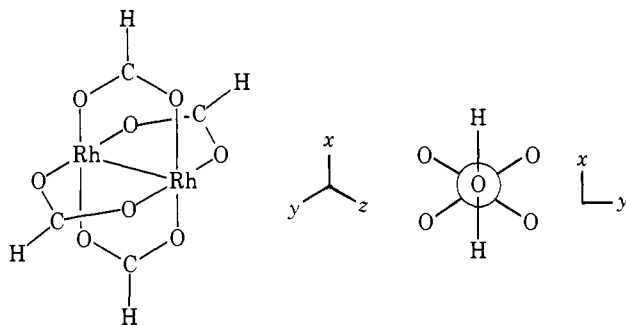
| Compd | M-M | M-L | Av M-O(COR) |
|------------------------------|-----------|-----------------------|-------------|
| $Mo_2(O_2CCF_3)_4^a$ | 2.090 (4) | 2.72 (1) ^e | 2.06 (2) |
| $Mo_2(O_2CCF_3)_4(py)_2^b$ | 2.129 (2) | 2.548 (8) | 2.116 (6) |
| $Rh_2(O_2CCH_3)_4(H_2O)_2^c$ | 2.386 (1) | 2.310 (3) | 2.039 (3) |
| $Cu_2(O_2CCH_3)_4(H_2O)_2^d$ | 2.615 (1) | 2.160 (3) | 1.969 (3) |

^a Reference 33. ^b Reference 28. ^c Reference 19. ^d Reference 20. ^e Intermolecular contact to carboxylate oxygen atom.

Table II. Sphere Radii (bohrs)^a and SCF Charge Distributions (electrons)

| Region ^b | $Rh_2(O_2CH)_4(H_2O)_2$ | | $Rh_2(O_2CH)_4$ | | Rh_2 | |
|---------------------|-------------------------|--------|-----------------|--------|--------|--------|
| | Radius | Charge | Radius | Charge | Radius | Charge |
| Rh | 2.481 | 44.26 | 2.450 | 44.09 | 2.503 | 44.22 |
| O | 1.736 | 7.98 | 1.703 | 7.88 | | |
| C | 1.618 | 5.23 | 1.587 | 5.14 | | |
| H | 1.316 | 0.96 | 1.292 | 0.93 | | |
| O _w | 1.774 | 8.02 | | | | |
| H _w | 1.163 | 0.74 | | | | |
| Intersphere | | 5.75 | | 6.39 | | 1.15 |
| Extramolecular | 8.894 | 0.18 | 8.294 | 0.14 | 5.064 | 0.41 |

^a 1 bohr = 0.529 177 Å. ^b O and O_w are carboxylate and water oxygen atoms, respectively, and similarly for the hydrogen atoms H and H_w.



$Rh_2(O_2CH)_4(H_2O)_2$, $Rh_2(O_2CH)_4$, and Rh_2 , respectively. The percentage for Rh_2 is the same as previously used³⁶ for Mo_2 . We believe that all the radii are within 0.1 bohr of the virial-theorem optimized values, although no effort was made to optimize them fully. The best values for $Rh_2(O_2CH)_4$ would probably be slightly larger than those for $Rh_2(O_2CH)_4(H_2O)_2$, rather than smaller as in the values used. Nothing in our experience suggests that any of the conclusions presented below would be altered by further refinement of the radii.

In other respects the calculations were carried out as previously described^{3,36} for $Mo_2(O_2CH)_4$ and Mo_2 . Ground-state SCF results were obtained for all three molecules. Since Rh_2 is predicted to be open shell, both spin-restricted and spin-polarized calculations of its lowest energy state were converged. Transition-state calculations were converged in spin-restricted form for the first two ionization energies of $Rh_2(O_2CH)_4(H_2O)_2$, and in spin-polarized form for all the spin- and dipole-allowed spectral transitions of Rh_2 .

Results

As for $Mo_2(O_2CH)_4$, the energy-level diagrams for $Rh_2(O_2CH)_4$ and $Rh_2(O_2CH)_4(H_2O)_2$ divide into three basic regions. The 20 essentially unperturbed formate C-H and C-O σ orbitals in the range -1.07 to -0.49 hartree have nearly the same energies in all three molecules. Four water-localized O-H bonding levels also lie in this region for the hydrated complex. In the range -0.43 to -0.21 hartree, $Rh_2(O_2CH)_4$ has 23 oxygen lone pair, C-O π , Rh-O, and Rh-Rh orbitals; two of a_{1g} , and one of a_{2u} , symmetry are found significantly perturbed in the hydrate (where a_{1g} and a_{2u} become a_g and b_{1u} , respectively) by interaction with the axial water molecules. Four

additional orbitals appear which correlate with H_2O σ and π lone pairs, the former being strongly mixed with Rh-Rh σ and σ^* functions. Above -0.18 hartree are found five unoccupied levels of Rh-Rh σ^* , Rh-O σ^* , and C-O π^* types, the first being significantly higher in energy in $Rh_2(O_2CH)_4(H_2O)_2$ than in $Rh_2(O_2CH)_4$ due to its simultaneous Rh-OH₂ σ^* character.

Energies and charge distributions for levels in the second and third regions are given in Table III. They are compared with those of free H_2O in Figure 1, with emphasis on levels important for discussion of the strength and trans influence of the Rh-Rh bond. Figure 2 compares the most important metal-metal and metal-water levels of $Rh_2(O_2CH)_4(H_2O)_2$ with their counterparts in $Mo_2(O_2CH)_4$. Wave function contour maps of critical H_2O -Rh-Rh-OH₂ σ and σ^* orbitals appear in Figures 3 and 4. The contours are the same as previously used^{2,3} for analogous orbitals in $Mo_2(O_2CH)_4$ and $Mo_2Cl_8^{4-}$. Table IV gives our assignment for the experimentally observed electronic spectrum of rhodium(II) carboxylates.

The SCF- $X\alpha$ -SW ground state of Rh_2 at Rh-Rh = 2.39 Å was explicitly determined by spin-restricted and spin-polarized calculations of all reasonable configurations. Spin-restricted eigenvalues for the state found to have lowest energy are compared in Figure 5 with those previously calculated³⁶ for Mo_2 at Mo-Mo = 2.10 Å. Figure 6 depicts the wave function for the interesting $2\sigma_g$ orbital of Rh_2 , essentially the 5s bonding combination; the contours are the same as previously used³ for the analogous orbital in Mo_2 . Table V compares the experimentally observed³⁴ electronic spectrum of Rh_2 with transitions which we calculate in the same energy range at Rh-Rh = 2.39 Å.

The calculated total energies for Rh_2 , $Rh_2(O_2CH)_4$, and $Rh_2(O_2CH)_4(H_2O)_2$ are -9371.8434, -10 127.0066, and -10 280.9064 hartrees, respectively. The corresponding virial ratios $-2T/V$ are 1.000 01, 1.000 30, and 1.000 11. Numbers of electrons in the various spatial regions are summarized in Table II.

Discussion

Strength of the Rh-Rh Bond. The calculations predict that the Rh-Rh bond in rhodium(II) carboxylates is single, not

Table III. Upper Valence Energy Levels (hartrees)^a and Charge Distribution for Rh₂(O₂CH)₄ and Rh₂(O₂CH)₄(H₂O)₂

| Rh ₂ (O ₂ CH) ₄ | | | | | | Rh ₂ (O ₂ CH) ₄ (H ₂ O) ₂ | | | | | | | | |
|--|---------------------|-----------------------|--------------------|--|-----------------|--|--|------------------|-----------------------|--------------------|-------------------|--|---------------------------------|------------------------------|
| D _{4h} level | Energy ^d | % charge ^b | | Major Rh basis Fns ^c | | Type | D _{2h} level | Energy | % charge ^b | | | Major Rh basis Fns ^c | | Type |
| | | 2Rh | 4O ₂ CH | | | | | | 2Rh | 4O ₂ CH | 2H ₂ O | | | |
| 7e _u | -0.0075 | 0 | 100 | | | C-O π* | 9b _{2u} | -0.0062 | 1 | 97 | 2 | | | C-O π* |
| 3b _{2g} | -0.0105 | 4 | 96 | | | | 9b _{3u} | -0.0065 | 1 | 97 | 2 | | | |
| 5b _{1g} | -0.1017 | 57 | 43 | d _{x²-y²} } | Rh-O σ* | Rh-O σ* | 6b _{1g} | -0.0959 | 58 | 42 | | d _{xy} } | Rh-O σ* | |
| 4b _{2u} | -0.1195 | 64 | 36 | | | | d _{x²-y²*}} | 5a _u | -0.1139 | 66 | 34 | | | |
| 4a _{2u} | -0.1756 | 82 | 18 | d _{z²*} | Rh-Rh σ* | Rh-Rh σ* | 8b _{1u} | -0.1359 | 78 | 14 | 8 | d _{z²*} | Rh-Rh σ*, Rh-OH ₂ σ* | |
| 2b _{1u} ^e | -0.2208 | 68 | 32 | d _{xy} * | Rh-Rh δ* | Rh-Rh δ* | 7b _{1u} ^e | -0.2161 | 70 | 30 | 0 | d _{x²-y²*} | Rh-Rh δ* | |
| 5e _g | -0.2343 | 84 | 16 | d _{xz,yz} * | Rh-Rh π* | Rh-Rh π* | 6b _{3g} | -0.2218 | 81 | 9 | 10 | d _{yz} * | Rh-Rh π* | |
| | | | | | | | | | 6b _{2g} | -0.2279 | 87 | | | 13 |
| 2b _{2g} | -0.2581 | 86 | 14 | d _{xy} | Rh-Rh δ | Rh-Rh δ | 9a _g | -0.2530 | 87 | 13 | 0 | d _{x²-y²} | Rh-Rh δ | |
| 6e _u | -0.2632 | 33 | 67 | d _{xz,yz} | Rh-O π, Rh-Rh π | Rh-O π, Rh-Rh π | 7b _{2u} | -0.2517 | 35 | 33 | 31 | d _{yz} | Rh-O π, Rh-Rh π | |
| | | | | | | | | | 7b _{3u} | -0.2614 | 38 | | | 61 |
| 1a _{1u} | -0.2803 | | 100 | | O lone pair | O lone pair | 8a _g | -0.2680 | 57 | 15 | 28 | d _{z²,s,p_z} } | Rh-Rh σ, Rh-OH ₂ σ* | |
| | | | | | | | 5b _{3g} | -0.2742 | 3 | 27 | 70 | | | |
| | | | | | | | 6b _{2u} | -0.2785 | 5 | 42 | 54 | | | H ₂ O π lone pair |
| 4e _g | -0.2906 | 11 | 89 | | O lone pair | O lone pair | 4a _u | -0.2811 | 0 | 100 | | } | O lone pair | |
| 5a _{1g} | -0.3008 | 50 | 50 | d _{z²,s} | Rh-O σ, Rh-Rh | Rh-O σ, Rh-Rh | 5b _{2g} | -0.2914 | 9 | 91 | 0 | | | |
| | | | | | | | | | 4b _{3g} | -0.2948 | 11 | | | 77 |
| 3e _g | -0.3038 | 11 | 89 | | O lone pair | O lone pair | 4b _{2g} | -0.3055 | 9 | 91 | 0 | } | Rh-Rh π, Rh-O π | |
| | | | | | | | 3b _{3g} | -0.3061 | 12 | 86 | 2 | | | |
| 5e _u | -0.3138 | 70 | 30 | d _{xz,yz} | Rh-Rh π, Rh-O π | Rh-Rh π, Rh-O π | 6b _{3u} | -0.3111 | 65 | 35 | 0 | d _{xz} } | Rh-Rh π, Rh-O π | |
| | | | | | | | | | 5b _{2u} | -0.3149 | 66 | | | 27 |
| 3a _{2u} | -0.3299 | 21 | 79 | d _{z²*,s*} } | Rh-O σ, π | Rh-O σ, π | 6b _{1u} | -0.3240 | 11 | 77 | 12 | d _{z²*,s*} } | Rh-O σ, π | |
| 3b _{2u} | -0.3405 | 26 | 74 | | | | d _{x²-y²*}} | 7a _g | -0.3355 | 18 | 67 | | | 15 |
| 1b _{1u} | -0.3533 | 39 | 61 | d _{xy} * | Rh-Rh σ, Rh-O σ | Rh-Rh σ, Rh-O σ | 3a _u | -0.3405 | 24 | 76 | 0 | d _{xy} * | Rh-O σ, π | |
| 4a _{1g} | -0.3561 | 66 | 34 | | | | d _{z²} | 5b _{1u} | -0.3549 | 37 | 63 | | | 0 |
| 4b _{1g} | -0.3589 | 40 | 60 | d _{x²-y²} } | Rh-O σ | Rh-O σ | 5b _{1g} | -0.3577 | 38 | 62 | | d _{xy} } | Rh-OH ₂ σ, Rh-Rh σ* | |
| 1a _{2g} | -0.3726 | | 100 | | | | | | | 4b _{1u} | -0.3712 | | | 16 |
| 4e _u | -0.3894 | 1 | 99 | | C-O π | C-O π | 4b _{1g} | -0.3738 | 0 | 100 | | } | C-O π | |
| | | | | | | | | | 5b _{3u} | -0.3917 | 1 | | | 99 |
| | | | | | | | 5b _{2u} | -0.3917 | 10199 | 0 | | | | |
| 1b _{2g} | -0.4228 | 17 | 83 | d _{xy} | Rh-OC π | Rh-OC π | 6a _g | -0.3932 | 44 | 3 | 53 | d _{z²} } | Rh-OH ₂ σ, Rh-Rh σ | |
| | | | | | | | | | 5a _g | -0.4260 | 16 | | | 84 |

^a All levels between -0.497 and -0.005 hartree except for diffuse Rydberg-state orbitals. These occur for Rh₂(O₂CH)₄(H₂O)₂ at -0.0602 (10a_g), -0.0459 (8b_{3u}), -0.0457 (8b_{2u}), -0.0432 (9b_{1u}), -0.0375 (11a_g), -0.0169 (7b_{2g}), and -0.0165 (7b_{3g}). Only 4-15% of their charge is located within the atomic spheres. A similar pattern is observed for Rh₂(O₂CH)₄. ^b Relative amounts of charge within the atomic spheres. The only Rh₂(O₂CH)₄(H₂O)₂ orbitals with less than 75% of the total charge within the atomic spheres are 9b_{2u} and 9b_{3u} (37%); the average is 84%. Rh₂(O₂CH)₄ is analogous. ^c Spherical harmonic basis functions contributing more than 10% of the Rh charge for important Rh-Rh, Rh-O(COH), and Rh-OH₂ orbitals, listed in order of decreasing importance. All such Rh contributions are more than 73% d except in 7a_g and 6b_{1u} for Rh₂(O₂CH)₄(H₂O)₂, and 5a_{1g} for Rh₂(O₂CH)₄, where they are ca. 40% s. Note that the difference in coordinate system between the two molecules makes d_{xy} in one analogous to d_{x²-y²} in the other, and vice versa. d_{xz} means a bonding d_{xz} combination, d_{z²*} an antibonding d_{z²} combination, etc. ^d 0.05 hartree has been added to the actual Rh₂(O₂CH)₄ eigenvalues. This shift makes the 20 formate-localized orbitals below -0.497 hartree (not tabulated here) essentially coincident with their counterparts in Rh₂(O₂CH)₄(H₂O)₂ and Mo₂(O₂CH)₄. ^e The highest occupied levels.

multiple. As shown by Figures 1 and 2, only the σ* orbital of the group σ, π, δ, δ*, π*, σ* remains empty. This is the same result one gets by naively adding six electrons to our diagram for Mo₂(O₂CH)₄. In moving from Mo to Rh, the M-O σ* and C-O π* orbitals which bracket the Mo-Mo σ* level are destabilized rather than stabilized relative to the metal-metal orbitals (see Figure 1). Moreover, no Rh 5s- or 5p-type orbitals (such as Cotton's σ_n pair) drop into the proper energy range. There is thus nothing to prevent occupation of the δ* and π* orbitals. The labeling of the levels in Figures 1 and 2 as purely

"σ", "σ*", etc., is of course an oversimplification; Table III shows their varying amounts of ligand character. Even considering all the orbitals of Rh₂(O₂CH)₄(H₂O)₂, however, one still finds a net excess of 2.0 Rh-Rh bonding over Rh-Rh antibonding electrons.

Our prediction of a single bond agrees with that made earlier from an extended-Hückel calculation.²² In some contrast to the extended-Hückel result, our calculated level ordering appears to be completely consistent with the experimental electronic spectrum, as discussed below. We thus feel that we have

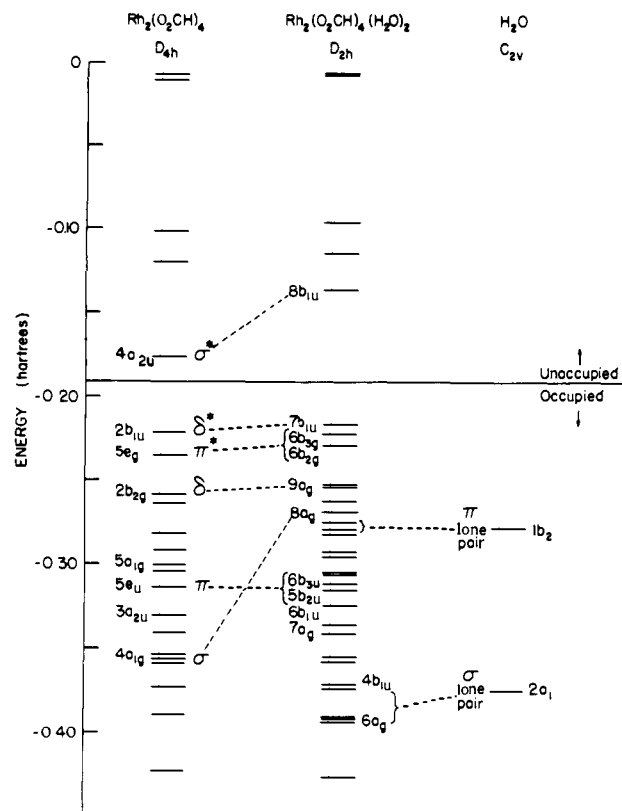


Figure 1. SCF energy levels for $\text{Rh}_2(\text{O}_2\text{CH})_4$, $\text{Rh}_2(\text{O}_2\text{CH})_4(\text{H}_2\text{O})_2$, and H_2O above -0.49 hartree. The levels which best correlate with the σ , π , δ , δ^* , π^* , and σ^* components of the Rh–Rh bond, and with the in- and out-of-plane water lone pairs, are indicated. Mulliken symbols are given for the Rh–Rh levels, and in addition for all other levels of Rh–Rh and/or Rh–OH₂ σ and σ^* character (a_{1g} and a_{2u} levels for $\text{Rh}_2(\text{O}_2\text{CH})_4$, a_g and b_{1u} for $\text{Rh}_2(\text{O}_2\text{CH})_4(\text{H}_2\text{O})_2$).

Table IV. Assignment of the Electronic Spectrum of $\text{Rh}_2(\text{O}_2\text{CCH}_3)_4(\text{H}_2\text{O})_2$

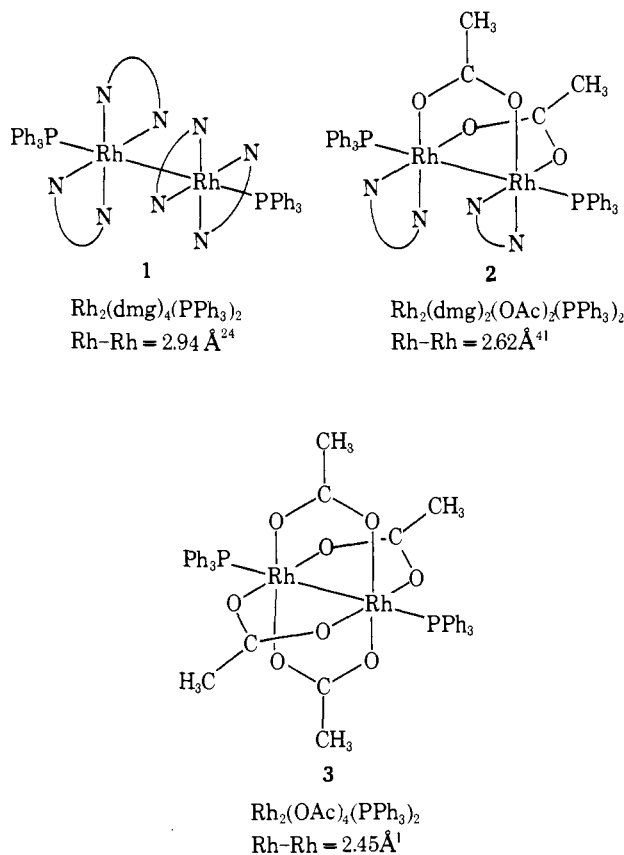
| D_{2h} transition | D_{4h} excited state | Type ^a | Exptl $\bar{\nu}_{\text{max}}$, $\text{cm}^{-1} \times 10^{-3}$ ^b |
|-------------------------------|------------------------|---|---|
| $6b_{3g} \rightarrow 8b_{1u}$ | 1E_u | $\pi^* \rightarrow \sigma^*$ | 17.1 (ϵ 241) |
| $6b_{2g} \rightarrow 5a_u$ | 1E_u | $\pi^* \rightarrow \text{Rh-O } \sigma^*$ | 22.7 (ϵ 106) |
| $8a_g \rightarrow 8b_{1u}$ | ${}^1A_{2u}$ | $\sigma \rightarrow \sigma^*$ | 40 sh (ϵ 4000) |
| $7a_g \rightarrow 8b_{1u}$ | ${}^1A_{2u}$ | $L\sigma \rightarrow \sigma^*$ | 45.9 (ϵ 17 000) |

^a σ , π , σ^* , and π^* denote the Rh–Rh character of mainly Rh orbitals. $L\sigma$ means a mainly formate orbital where the Rh–O(COH) and Rh–Rh interactions are σ . ^b Bond maxima and molar absorptivities in aqueous solution at room temperature, from ref 27.

placed the prediction of bond order on a much firmer foundation.

As noted earlier, the observed Rh–Rh distance of 2.39 Å in $\text{Rh}_2(\text{O}_2\text{CCH}_3)_4(\text{H}_2\text{O})_2$ seems short for a single bond, by comparison to other known Rh–Rh distances and estimates of covalent radii. One may argue that such covalent radii are well known to be ligand dependent;³⁷ in particular, most of the known Rh–Rh single bonds occur between metal atoms in lower oxidation states than in the acetate, and thus involve “larger” atoms. However, this effect seems unlikely to account for the entire shortening of the acetate distance from, e.g., that of 2.73 Å in $\text{Rh}_4(\text{CO})_{12}$.³⁸ The natural inference is that the bridging carboxylate ligands constrain the metals to a shorter separation than they would otherwise prefer. The O···O distance in sodium formate is 2.22 Å;³⁹ this presumably ap-

proximates the ideal metal–metal separation from the viewpoint of the formate ligand. Metal–metal distances of 2.09–2.72 Å are known—and can thus be accommodated—within the $\text{M}_2(\text{O}_2\text{CR})_4$ framework, but this does not prove that these distances would not be different if the C–O distance and/or O–C–O angle were perfectly flexible. The weaker a metal–metal bond, the more likely it is to be affected by ligand preferences.⁴⁰



The three structures below relate to this question. We believe that **1**, **2**, and **3** all contain Rh–Rh single bonds. No one has ever asserted otherwise for **1**.²⁴ Details of the crystal structure strongly support the idea that the ca. 0.2 Å elongation over the usual Rh–Rh distance is due to repulsion between the parallel dimethylglyoximate ligands. To us, this indicates how flexible the Rh–Rh single bond is to such ligand effects. In **2**, we see the dmgl–dmgl repulsion as approximately balanced by the constraining effect of the bridging acetates, leading to a Rh–Rh distance only a little shorter than normal. The distance in **3** reflects the full constraint of the acetate cage.⁴²

Synthesis and structural characterization of Rh_2^{4+} systems with a greater variety of bridging and nonbridging ligands are needed to fully clarify the question of bridge constraint. Our own initial efforts in this direction have not been successful;⁴³ we hope that the above discussion will stimulate others to work in this area.

Mutual Influence of the Rh–Rh and Rh–OH₂ Bonds. Figure 1 and Table III show that the interaction of H_2O with $\text{Rh}_2(\text{O}_2\text{CH})_4$ is essentially of σ type. Not only mainly formate levels, but also the π , π^* , δ , and δ^* Rh–Rh orbitals, have nearly identical energies in $\text{Rh}_2(\text{O}_2\text{CH})_4$ and $\text{Rh}_2(\text{O}_2\text{CH})_4(\text{H}_2\text{O})_2$. The same is true for the water π lone-pair orbitals relative to free water. A contour map of the one Rh–Rh π -type orbital with appreciable H_2O character, $7b_{2u}$, shows that no significant Rh–OH₂ overlap accompanies this mixing. The small amount of H_2O character found in the $6b_{3g}$ (Rh–Rh π^*) orbital, 10%, is quite consistent with results of an EPR study of $\text{Rh}_2(\text{O}_2\text{CCF}_3)_4$ –nitroxide adducts.⁴⁴

Table V. Experimental Electronic Spectrum of Rh₂, Compared with Transitions Calculated at Rh-Rh = 2.39 Å

| Transition ^a | Calcd energy, cm ⁻¹ × 10 ⁻³ | Exptl $\bar{\nu}_{\max}$, cm ⁻¹ × 10 ⁻³ ^b |
|---------------------------------------|--|--|
| (2σ _g → 2σ _u)↑ | 21.7 | |
| (1σ _g → 1σ _u)↓ | 24.4 | |
| (1π _g → 2σ _u)↑ | 25.2 | 29.1 |
| (2σ _g → 2π _u)↑ | 25.3 | 30.8 |
| (1π _g → 2π _u)↑ | 29.8 | 31.5 |
| (1δ _g → 2π _u)↓ | 34.8 | 32.1 |
| (1δ _g → 2π _u)↑ | 39.3 | |

^a All spin- and dipole-allowed transitions between 17 and 44 × 10⁻³ cm⁻¹. Vertical arrows indicate whether levels involved are spin-up or spin-down. ^b In an Ar matrix at 10 K, from ref 34. Note that large regions of the spectrum are obscured by strong Rh-atom absorptions.

The symmetric combination of the two H₂O σ lone pair orbitals interacts with the Rh-Rh σ orbitals (4a_{1g} and 5a_{1g}); the antisymmetric combination interacts with the Rh-Rh σ* orbitals (3a_{2u} and unoccupied 4a_{2u}). The two original Rh₂(O₂CH)₄ orbitals, and the three of Rh₂(O₂CH)₄(H₂O)₂ which result, are depicted for both cases in Figures 3 and 4. The lowest of the three, most like the H₂O lone pairs, are Rh-OH₂ bonding; the highest, the main Rh-Rh σ and σ* orbitals, are Rh-OH₂ antibonding; the middle pair are mainly formate and hence approximately Rh-OH₂ nonbonding. The point is that metal-metal bonding weakens both of the metal-water interactions. In a_{1g} symmetry, it stabilizes the Rh-Rh σ orbital so that it becomes fully occupied. Thus both the bonding and antibonding Rh-OH₂ a_g orbitals end up filled, and little, if any, net bonding results. Similarly, in a_{2u} symmetry, Rh-Rh bonding destabilizes the Rh-Rh σ* orbital, so that it is further away in energy, and thus interacts more weakly, with the water lone pairs than it would if the Rh-Rh bond were absent. Thus we can see both why the metal-water bond is weaker than normal, and why bonds to trans ligands get weaker as the metal-metal bond gets stronger: the stronger the metal-metal bond, the higher in energy the σ* orbital will be. The extremely long Mo-N distance of 2.55 Å in Mo₂(O₂CCF₃)₄(py)₂ is thus seen as a necessary consequence of the very strong Mo-Mo σ bond (see Figure 2).

This orbital picture of the trans influence emphasizes its mutual nature: ligands trans to the metal-metal bond will always be more weakly bound than normal, but they in turn will always weaken the metal-metal bond somewhat. As Figure 3 shows, the net effect of the H₂O molecules on the Rh-Rh σ orbitals is a small shift of Rh-Rh bonding electrons to higher energy, corresponding to a weakening of the Rh-Rh bond. The effect is not as dramatic as Figure 1 might indicate, since only the *most important* Rh-Rh σ orbitals are connected there. More significant for the Rh-Rh bond weakening, and not clear from Figure 1, is the influence of H₂O on the Rh-Rh σ* system. Figure 4 shows that, in contrast to the σ system, the upper two b_{1u} orbitals of Rh₂(O₂CH)₄(H₂O)₂ correlate very directly with the original two a_{2u} orbitals of Rh₂(O₂CH)₄. The presence of the "extra" 4b_{1u} orbital in the hydrate thus corresponds to a shift of Rh-Rh antibonding electrons to lower energy. It should be kept in mind that our calculated difference in Rh-Rh bond strength between Rh₂(O₂CH)₄ and Rh₂(O₂CH)₄(H₂O)₂ represents a lower limit, since we have kept the Rh-Rh distance in the former at the experimental value for the latter, 2.39 Å.

Experimental facts confirm the competitive nature of metal-metal and metal-trans ligand bonds. In Rh₂(O₂CCH₃)₄(PPh₃)₂, the Rh-P bonds of 2.48 Å are ca. 0.15 Å longer than normal.²⁵ This lengthening is not as great as for the Rh-OH₂ bonds in the hydrate (ca. 0.27 Å¹⁹); PPh₃ is ap-

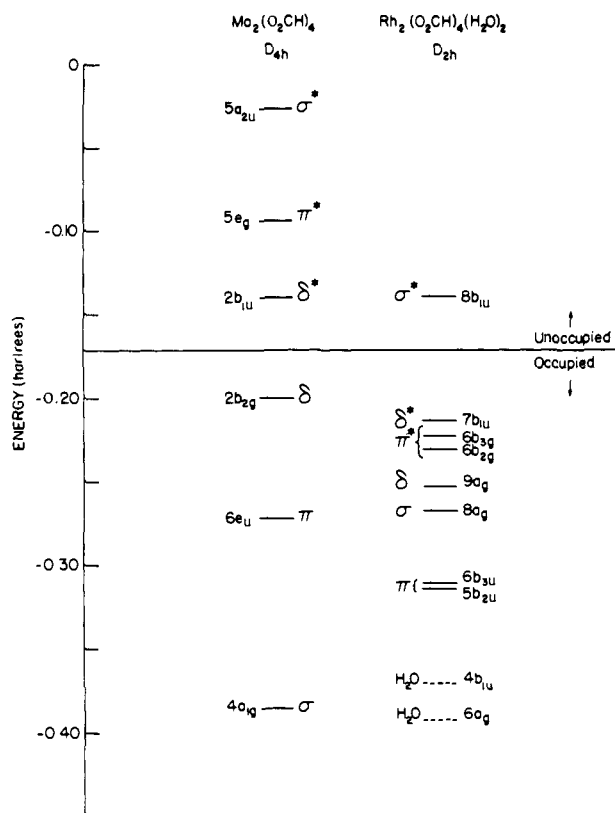


Figure 2. Most important energy levels of Mo₂(O₂CH)₄ and Rh₂(O₂CH)₄(H₂O)₂ for metal-metal and metal-water bonding. The symbols σ, π, δ, δ*, π*, and σ* refer to metal-metal character. For metal-water interaction, 6a_g and 4b_{1u} have σ character, while 8a_g and 8b_{1u} are σ*.

parently better than H₂O at competing with the other Rh atom as a ligand. Consequently, the Rh-Rh bond is 0.06 Å longer than in the hydrate. Similar comparisons^{45a} hold for Mo₂(O₂CCF₃)₄ and Mo₂(O₂CCF₃)₄(py)₂ (see Table I); for Cr₂(O₂CCH₃)₄ and Cr₂(O₂Cch₃)₄(H₂O)₂;^{45b} and for Re₂Cl₈²⁻ and Re₂Cl₈(H₂O)₂²⁻.^{45c}

Rh₂(O₂CH)₄(H₂O)₂ and Mo₂(O₂CH)₄. The chief difference between the energy levels of these two molecules not already noted is the general downshift of mainly d levels in the Rh case—in contrast to the mainly formate levels, which remain at virtually the same energies. The exception is, of course, the main metal-metal σ orbital, destabilized by the water interaction so that it even lies above the π orbital (see Figure 2).

This downshift is due to the greater electronegativity of Rh than Mo. A consequence is greater ligand character in the ten mainly d orbitals; they average 81% Mo, but only 71% Rh. This does not imply significantly more covalent metal-formate oxygen bonds; the eight M-O bonding orbitals are 27% Rh, compared to 25% Mo. The extra attraction of the metal for electrons is thus used almost entirely in binding the two H₂O molecules.

Electronic Spectra of Rh₂⁴⁺ and Rh₂⁵⁺ Complexes. The electronic spectrum of rhodium(II) acetate in water consists of two weak bands in the visible region and two stronger bands, the first a shoulder on the second, in the ultraviolet.²⁷ As the axial water ligands are replaced by stronger donors, band I shifts uniformly to higher energy, while band II remains relatively constant. Bands III and IV shift to lower energies, the former faster than the latter.²² We have not done transition-state calculations of the spectrum, and so have no absolutely quantitative predictions of transition energies to offer. An entirely reasonable assignment, however, emerges from ground-state energy differences, the magnitudes of relaxation

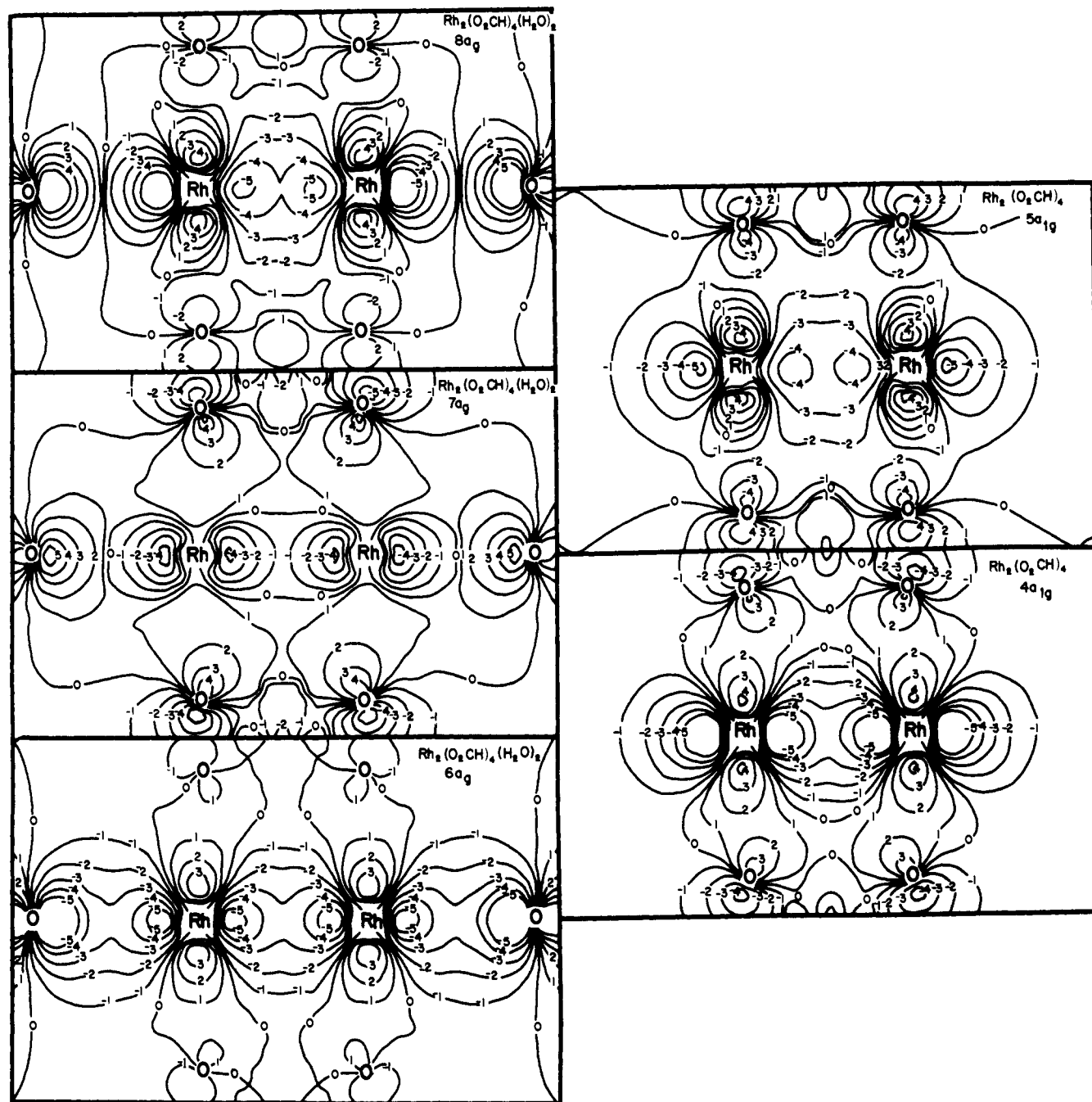


Figure 3. Contour maps of the wave functions for the important Rh-Rh σ levels of $\text{Rh}_2(\text{O}_2\text{CH})_4(\text{H}_2\text{O})_2$ and $\text{Rh}_2(\text{O}_2\text{CH})_4$, showing the bonding of the trans H_2O molecules in a_g symmetry. These maps and those of Figure 4 are in the plane of two of the formate groups, with contour values of 0, ± 1 , ± 2 , ± 3 , ± 4 , $\pm 5 = 0$, ± 0.02 , ± 0.05 , ± 0.09 , ± 0.13 , ± 0.17 , respectively. Interior contours close to the atomic centers are always omitted for clarity.

we expect from experience for various types of transitions, and the above experimental observations; it is given in Table IV. We consider only transitions allowed in D_{4h} symmetry.

The predicted spectrum begins with two distinct transitions, $\pi^* \rightarrow \sigma^*$ and $\pi^* \rightarrow \text{Rh-O } \sigma^*$. The ground-state energy differences are 19.5 and $24.4 \times 10^{-3} \text{ cm}^{-1}$, respectively. These are close to the experimental positions of bands I and II, 17.1 and $22.7 \times 10^{-3} \text{ cm}^{-1}$, respectively, and we expect little relaxation in the transition state. Moreover, taking the comparison between $\text{Rh}_2(\text{O}_2\text{CH})_4$ and $\text{Rh}_2(\text{O}_2\text{CH})_4(\text{H}_2\text{O})_2$ in Figure 1 as indicative of changes when the axial-ligand donor strength is increased, we see that $\pi^* \rightarrow \sigma^*$ should go up while $\pi^* \rightarrow \text{Rh-O } \sigma^*$ remains constant. Finally, the essentially d \rightarrow d character of both transitions suggests that they should be weaker than an ordinary allowed excitation. The complete consistency of these predictions with experiment gives us

confidence that we have correctly assigned bands I and II.

Nine allowed transitions have energies fairly close to those of bands III and IV. However, only two of these should show the observed red shift as axial donor strength increases. The reason, again referring to Figure 1, is that only Rh-Rh σ -type orbitals are significantly elevated in energy by the axial donors. For this purpose one should associate $8a_g$ and $7a_g$ in the hydrate with $5a_{1g}$ and $4a_{1g}$ in $\text{Rh}_2(\text{O}_2\text{CH})_4$, respectively. The only allowed transitions of reasonable energy originating in $8a_g$ and $7a_g$ terminate in $8b_{1u}$, the Rh-Rh σ^* orbital. We thus assign band III to $8a_g \rightarrow 8b_{1u}$ and band IV to $7a_g \rightarrow 8b_{1u}$. As expected from the considerable ligand to metal charge transfer in the predicted transitions, more for the second than the first, the intensities of bands III and IV are greater than for bands I and II, band IV being stronger than band III. The ground-state energy difference for $7a_g \rightarrow 8b_{1u}$, $43.8 \times 10^{-3} \text{ cm}^{-1}$, is close

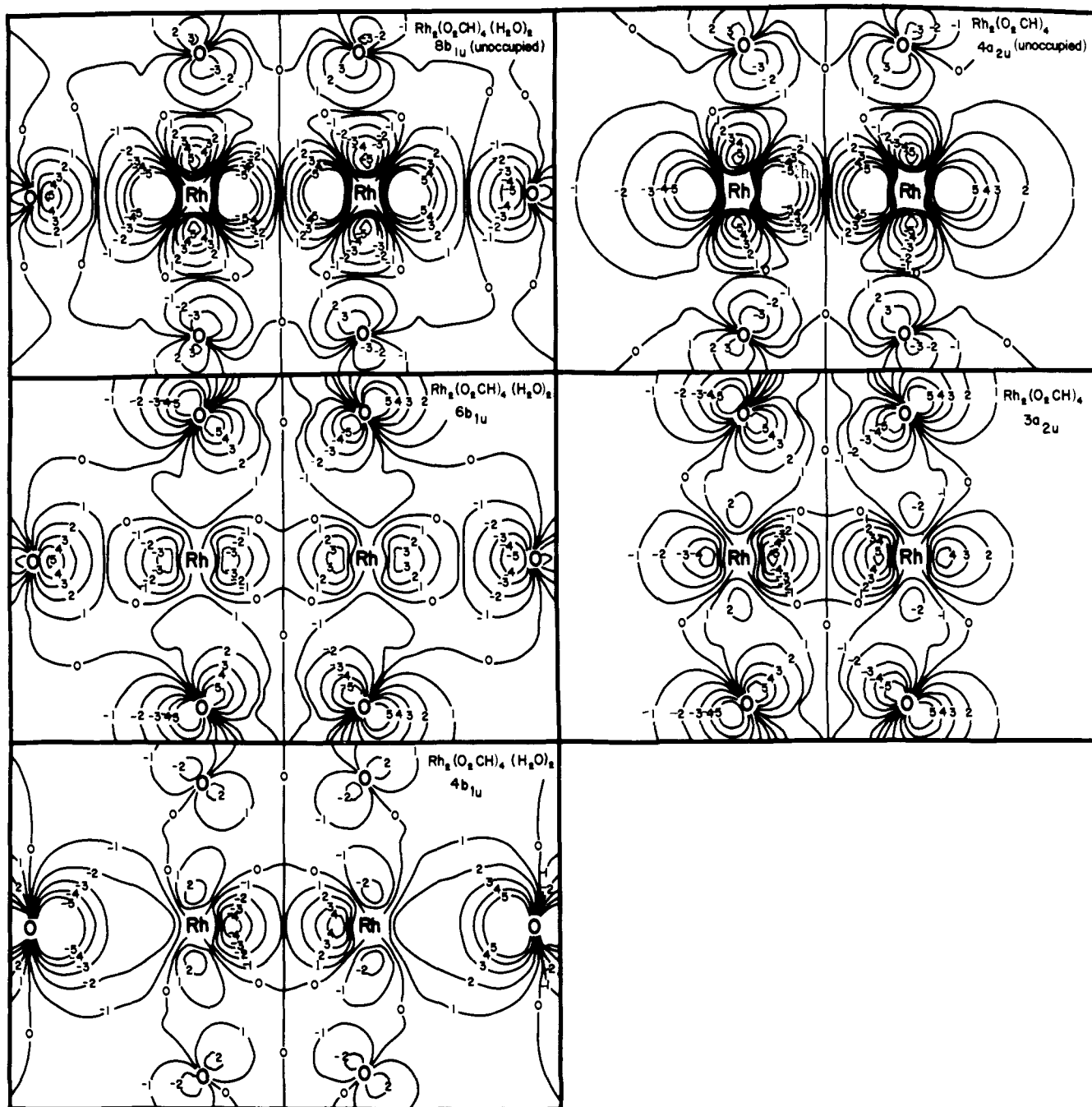


Figure 4. Contour maps of the wave functions for the important Rh-Rh σ^* levels of $\text{Rh}_2(\text{O}_2\text{CH})_4(\text{H}_2\text{O})_2$ and $\text{Rh}_2(\text{O}_2\text{CH})_4$, showing the bonding of the trans H_2O molecules in b_{1u} symmetry.

the experimental energy of band IV, $45.9 \times 10^{-3} \text{ cm}^{-1}$. The low ground-state value for $8a_g \rightarrow 8b_{1u}$, 29.0 compared to 40 for band III, is not surprising since this is essentially the Rh-Rh $\sigma \rightarrow \sigma^*$ transition, and thus should show very great ground to transition state relaxation.

Our assignment of bands I, II, and III parallels that of Dubicki and Martin based on an extended-Hückel calculation.²² Their arguments were based more on using the calculation as a rough guide to interpret the spectral changes caused by different axial ligands since, e.g., the extended-Hückel diagram would predict the $\pi^* \rightarrow \text{Rh-O } \sigma^*$ transition at lower energy than $\pi^* \rightarrow \sigma^*$. Their assignment of band IV corresponds in our scheme to $6b_{1u} \rightarrow 11a_g$ ($L\sigma^* \rightarrow \text{Rydberg}$); we consider this unlikely as our calculated ground-state energy difference is $62.9 \times 10^{-3} \text{ cm}^{-1}$.

The spectra of $\text{Rh}_2(\text{CO}_3)_4^{4-}$, $\text{Rh}_2(\text{SO}_4)_4^{4-}$, and

$\text{Rh}_2(\text{H}_2\text{O})_{10}^{4+}$ are so similar to that of rhodium(II) acetate²⁷ that we propose an entirely analogous assignment, and a similar electronic structure in general, for them. Noteworthy is the downshift of the metal-metal bands for $\text{Rh}_2(\text{H}_2\text{O})_{10}^{4+}$ relative to the acetate, as expected if the Rh-Rh bond has lengthened upon replacing bridging acetate with nonbridging water ligands.

The solution spectrum of the ephemeral ion $[\text{Rh}_2(\text{O}_2\text{CCH}_3)_4]^+$ also closely resembles that of the neutral species, with the addition of a new low-energy band at $12.3 \times 10^{-3} \text{ cm}^{-1}$ (ϵ 476).^{27,46} We tentatively suggest that this is the $\delta \rightarrow \delta^*$ transition ($9a_g \rightarrow 7b_{1u}$), made possible by the removal of one δ^* electron upon ionization. Another possibility is $7b_{2,3u} \rightarrow 6b_{2,3g}$ ($\pi \rightarrow \pi^*$), if π^* rather than δ^* is the HOMO. Our spin-restricted transition-state calculations give ionization energies of 8.23 and 8.41 eV for the $7b_{1u}(\delta^*)$ and $6b_{3g}(\pi^*)$

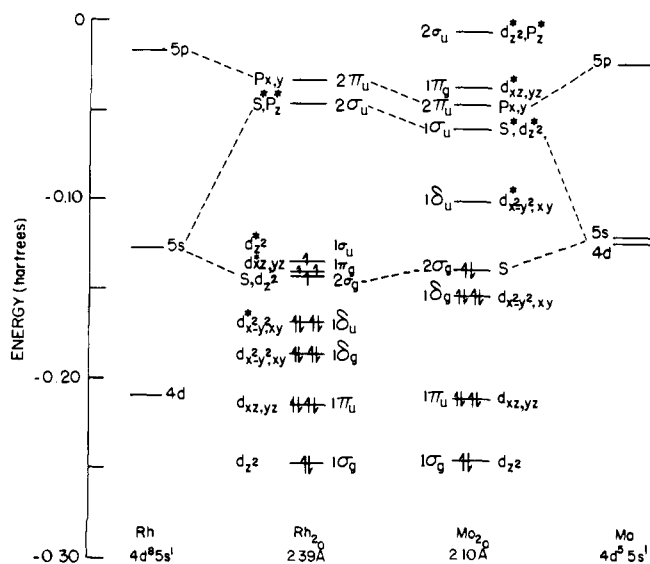


Figure 5. Spin-restricted valence energy levels for Rh_2 , Mo_2 , Rh , and Mo . Analogous spin-polarized levels for Rh_2 exhibit spin-spin splittings averaging 0.043 hartree, the $1\sigma_g$ level being at -0.264 hartree. Levels of Rh_2 and Mo_2 which best correlate with $5s$ and $5p$ atomic orbitals are connected by dashed lines; all other levels best correlate with $4d$ orbitals. $d_{x^2-y^2}$ refers to a degenerate bonding combination of d_{x^2} or d_{y^2} orbitals, d_{z^2} to a nondegenerate antibonding combination of d_{z^2} orbitals, etc.

orbitals, respectively, of $Rh_2(O_2CH)_4(H_2O)_2$, thus predicting that δ^* remains highest in the positive ion. We do not consider that we can very firmly predict the HOMO for either neutral acetate or its ion, however, in view of the close spacing, previous difficulty in accurately defining the δ^* position,^{3a} and possible small differences between the formate and acetate.

Rh_2 and Mo_2 . The recent measurements of electronic spectra and other properties for transition-metal diatomics such as Sc_2 ,⁴⁷ Ti_2 ,⁴⁷ V_2 ,⁴⁸ Nb_2 ,⁴⁹ Cr_2 ,^{36,50} Mo_2 ,^{36,49} $CrMo$,³⁶ Ni_2 ,⁵¹ and Rh_2 ³⁴ in Ar matrices at low temperature provide experimental access to the interesting and fundamental phenomenon of strong bonds between two metal atoms in the complete absence of ligands. We have previously presented some SCF- $X\alpha$ -SW results for Cr_2 , $CrMo$, and Mo_2 , including a very successful assignment of their measured electronic spectra.^{3a,36} Here we briefly compare our initial ground-state calculations on Rh_2 with those on Mo_2 .

The " $d^{10}s^2$ " valence configuration found for Mo_2 is just a doubling of the d^5s^1 configuration of the atom. In contrast, as shown in Figure 5, dimerization of Rh apparently leads to replacement of one s by one d electron; the configuration is " $d^{17}s^1$ ". This is a result of the smaller d -band splitting in Rh_2 (that for Mo_2 is still about 50% greater even if $Mo-Mo = 2.39$ Å is used), and the downshift of $4d$ relative to $5s$ orbitals, which leaves the s -type $2\sigma_g$ and d -type $1\pi_g$ and $1\sigma_u$ in such proximity as to favor an open-shell $S = 2$ ground state. Despite the contraction of the d orbitals, the net bonding is still largely d in character.⁵² Naive subtraction of antibonding from bonding electrons leaves a net bond order of two, compared to six in Mo_2 . Comparison of Figure 6 with its counterpart (Figure 7) in ref 3a shows the effect of the ca. 10% d_{z^2} character which the mainly s orbital has acquired in Rh_2 . It remains, however, much more diffuse than the d -like orbitals; note the smaller contours required for good resolution than in Figures 3 and 4.

These conclusions are likely to remain valid for a fair range of $Rh-Rh$ distances around 2.39 Å. As yet we have neither an experimental nor theoretical estimate of the actual bond distance. The former is unlikely to appear in the near future; we intend to investigate the latter problem through calculations at several bond distances, using the $X\alpha$ -SW total energy and

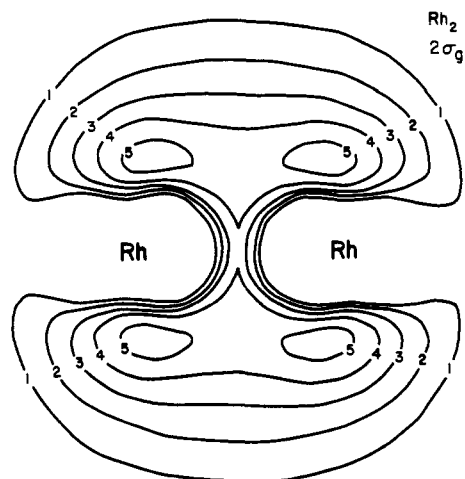


Figure 6. Contour map of the wave function for the $2\sigma_g$ level of Rh_2 at $Rh-Rh = 2.39$ Å. The contour values are 0, 1, 2, 3, 4, 5 = 0, 0.02, 0.03, 0.04, 0.05, 0.06, respectively.

comparisons of the calculated and experimental electronic spectrum as guides. As shown in Table V, the 2.39 Å calculation of the spectrum does not yield a clear assignment. Qualitative consideration of how the predicted transition energies would change with distance does, however, suggest that such an assignment may emerge from the transitions listed in Table V at some other distance. Whether this will actually occur, and whether at a large or smaller distance, remains to be seen.

$Ru(2.5)$ Carboxylates. Dinuclear ruthenium carboxylates are unique among this class of compounds in being stable as positive ions and highly paramagnetic (three unpaired electrons).⁵³ $[Ru_2(O_2CC_3H_7)_4]Cl$ exhibits $Ru-Ru = 2.28$ Å,¹⁷ intermediate between the metal-metal distances of 2.09 and 2.39 Å in molybdenum(II) and rhodium(II) carboxylates. We recall that the basic electronic structure of $Rh_2(O_2CH)_4(H_2O)_2$ is generated merely by adding six electrons to the $X\alpha$ -SW diagram for $Mo_2(O_2CH)_4$ (see Figure 2). This suggests that the ground state of $[Ru_2(O_2CR)_4]Cl$ is $\sigma^2\pi^4\delta^2\pi^*2\delta^*1$, the open-shell character resulting from close spacing of the π^* and δ^* orbitals.⁵⁴ Our $X\alpha$ -SW calculations on $[Ru_2(O_2CH)_4]Cl$ have proceeded far enough to explicitly confirm this suggestion. Details will appear in a latter publication.⁵⁵

Acknowledgment. We thank the National Science Foundation for support of this research.

References and Notes

- (1) F. A. Cotton, *Chem. Soc. Rev.*, **4**, 27 (1975).
- (2) J. G. Norman, Jr., and H. J. Kolari, *J. Am. Chem. Soc.*, **97**, 33 (1975); *J. Chem. Soc., Chem. Commun.*, 303 (1974).
- (3) (a) J. G. Norman, Jr., H. J. Kolari, H. B. Gray, and W. C. Troglor, *Inorg. Chem.*, **16**, 987 (1977); (b) J. G. Norman, Jr., and H. J. Kolari, *J. Chem. Soc., Chem. Commun.*, 649 (1975).
- (4) A. P. Mortola, J. W. Moskowitz, N. Rosch, C. D. Cowman, and H. B. Gray, *Chem. Phys. Lett.*, **32**, 283 (1975).
- (5) F. A. Cotton and G. G. Stanley, *Inorg. Chem.*, **16**, 2668 (1977).
- (6) (a) C. D. Garner, I. H. Hillier, M. F. Guest, J. C. Green, and A. W. Coleman, *Chem. Phys. Lett.*, **41**, 91 (1976); (b) M. F. Guest, I. H. Hillier, and C. D. Garner, *ibid.*, **48**, 587 (1977).
- (7) M. Benard and A. Veillard, *Nouveau J. Chim.*, **1**, 97 (1977).
- (8) L. Dubicki and R. L. Martin, *Aust. J. Chem.*, **22**, 1571 (1969).
- (9) (a) F. A. Cotton, B. A. Frenz, B. R. Stults, and T. R. Webb, *J. Am. Chem. Soc.*, **98**, 2768 (1976); (b) F. A. Cotton, D. S. Martin, T. R. Webb, and T. J. Peters, *Inorg. Chem.*, **15**, 1199 (1976); (c) F. A. Cotton, D. S. Martin, P. E. Fanwick, T. J. Peters, and T. R. Webb, *J. Am. Chem. Soc.*, **98**, 4681 (1976).
- (10) (a) C. D. Cowman and H. B. Gray, *J. Am. Chem. Soc.*, **95**, 8177 (1973); (b) W. C. Troglor, C. D. Cowman, H. B. Gray, and F. A. Cotton, *ibid.*, **99**, 2993 (1977); (c) W. C. Troglor, E. I. Solomon, I. Trajberg, C. J. Ballhausen, and H. B. Gray, *Inorg. Chem.*, **16**, 828 (1977); (d) D. K. Erwin, G. L. Geoffrey, H. B. Gray, G. S. Hammond, E. I. Solomon, W. C. Troglor, and A. A. Zagars, *J. Am. Chem. Soc.*, **99**, 3620 (1977).

- (11) J. San Filippo and H. J. Sniadoch, *Inorg. Chem.*, **15**, 2209 (1976).
 (12) A/ P. Sattelberger and J. P. Fackler, *J. Am. Chem. Soc.*, **99**, 1258 (1977).
 (13) J. C. Green and A. J. Hayes, *Chem. Phys. Lett.*, **31**, 306 (1975).
 (14) F. A. Cotton, J. G. Norman, Jr., B. R. Stults, and T. R. Webb, *J. Coord. Chem.*, **5**, 217 (1976).
 (15) R. J. H. Clark and M. L. Franks, *J. Am. Chem. Soc.*, **97**, 2691 (1975); **98**, 2763 (1976).
 (16) F. A. Cotton and E. Pedersen, *J. Am. Chem. Soc.*, **97**, 303 (1975).
 (17) M. J. Bennett, K. G. Caulton, and F. A. Cotton, *Inorg. Chem.*, **8**, 1 (1969).
 (18) J. Drew, M. B. Hursthouse, P. Thornton, and A. J. Welch, *J. Chem. Soc., Chem. Commun.*, 52 (1973).
 (19) F. A. Cotton, B. G. DeBoer, M. D. LaPrade, J. R. Pipal, and D. A. Ucko, *Acta Crystallogr., Sect. B*, **27**, 1664 (1971).
 (20) (a) R. Chidambaram and G. M. Brown, *Cryst. Struct. Commun.*, **1**, 269 (1972); (b) P. de Meester, S. R. Fletcher, and A. C. Skapski, *J. Chem. Soc., Dalton Trans.*, 2575 (1973).
 (21) M. A. Porai-Koshits and A. S. Antsyshkina, *Dokl. Chem.*, **146**, 902 (1962).
 (22) L. Dubicki and R. L. Martin, *Inorg. Chem.*, **9**, 673 (1970).
 (23) F. A. Cotton, *Acc. Chem. Res.*, **2**, 240 (1969).
 (24) An exception, where ligand–ligand repulsions appear quite severe, is described in K. G. Caulton and F. A. Cotton, *J. Am. Chem. Soc.*, **93**, 1914 (1971).
 (25) F. A. Cotton and J. G. Norman, Jr., *J. Am. Chem. Soc.*, **93**, 80 (1971).
 (26) SCF– X_{α} –SW calculations on $Tc_2Cl_8^{3-}$ (F. A. Cotton and B. J. Kalbacher, *Inorg. Chem.*, **16**, 2386 (1977) and EPR experiments on Re analogues (ref 16) place the unpaired electron in the δ^* , not a σ_n , orbital.
 (27) C. R. Wilson and H. Taube, *Inorg. Chem.*, **14**, 405, 2276 (1975).
 (28) F. A. Cotton and J. G. Norman, Jr., *J. Am. Chem. Soc.*, **94**, 5697 (1972).
 (29) A. Pidcock, R. E. Richards, and L. M. Venanzi, *J. Chem. Soc. A*, 1707 (1966).
 (30) T. G. Appleton, H. C. Clark, and R. E. Manzer, *Coord. Chem. Rev.*, **10**, 335 (1973).
 (31) E. M. Shustorovich, M. A. Porai-Koshits, and Y. A. Buslaev, *Coord. Chem. Rev.*, **17**, 1 (1975).
 (32) R. Mason and A. D. C. Towl, *J. Chem. Soc. A*, 1601 (1970).
 (33) F. A. Cotton and J. G. Norman, Jr., *J. Coord. Chem.*, **1**, 161 (1972).
 (34) L. A. Hanlan and G. A. Ozin, *Inorg. Chem.*, **16**, 2848 (1977).
 (35) J. G. Norman, Jr., *J. Chem. Phys.*, **61**, 4630 (1974); *Mol. Phys.*, **31**, 1191 (1976).
 (36) W. Klotzbücher, G. A. Ozin, J. G. Norman, Jr., and H. J. Kolari, *Inorg. Chem.*, **16**, 2871 (1977).
 (37) R. Mason, *Chem. Soc. Rev.*, **1**, 431 (1972).
 (38) C. H. Wei, *Inorg. Chem.*, **8**, 2384 (1969).
 (39) P. L. Markila, S. J. Rettig, and J. Trotter, *Acta Crystallogr., Sect. B*, **31**, 2927 (1975).
 (40) R. H. Summerville and R. Hoffmann, *J. Am. Chem. Soc.*, **98**, 7240 (1976).
 (41) J. Halpern, E. Kimura, J. Molin-Case, and C. S. Wong, *Chem. Commun.*, 1207 (1971).
 (42) We note here that this analysis places one of us (J.G.N.) in the interesting position of refuting the conclusions of his first scientific paper (ref 25).
 (43) J. G. Norman, Jr., and E. O. Fey, *J. Chem. Soc., Dalton Trans.*, 765 (1976).
 (44) R. M. Richman, T. C. Kuechler, S. P. Tanner, and R. S. Drago, *J. Am. Chem. Soc.*, **99**, 1055 (1977).
 (45) (a) As part of an analysis of quadruply bonded structures, others recently gave a qualitative discussion of the metal–metal trans influence which includes many of the same ideas we have presented above (D. M. Collins, F. A. Cotton, and C. A. Murillo, *Inorg. Chem.*, **15**, 1861 (1976)); (b) F. A. Cotton, C. E. Rice, and G. W. Rice, *J. Am. Chem. Soc.*, **99**, 4704 (1977); (c) F. A. Cotton and W. T. Hall, *Inorg. Chem.*, **16**, 1867 (1977).
 (46) R. D. Cannon, P. B. Powell, K. Sarawek, and J. S. Stillman, *J. Chem. Soc., Chem. Commun.*, 31 (1976).
 (47) R. Busby, W. Klotzbücher, and G. A. Ozin, *J. Am. Chem. Soc.*, **98**, 4013 (1976).
 (48) T. A. Ford, H. Huber, W. Klotzbücher, E. P. Kundig, M. Moskovits, and G. A. Ozin, *J. Chem. Phys.*, **66**, 524 (1977).
 (49) W. Klotzbücher and G. A. Ozin, *Inorg. Chem.*, **16**, 984 (1977).
 (50) E. P. Kundig, M. Moskovits, and G. A. Ozin, *Nature (London)*, **254**, 503 (1975).
 (51) M. Moskovits and J. E. Hulse, *J. Chem. Phys.*, **66**, 3988 (1977).
 (52) This contrasts sharply with Ni_2 , where the bond is found to be essentially s in character by both GVB (c. F. Melius, J. W. Moskowitz, A. P. Mortola, M. B. Baillie, and M. A. Ratner, *Surf. Sci.*, **59**, 279 (1976)) and X_{α} –SW (K. H. Johnson, personal communication) calculations. One expects d orbitals to increase in importance relative to s orbitals as one moves down a column (Ni_2 to Rh_2) or to the left in a row (Ni_2 to Cr_2 and Mo_2). The former phenomenon has been explicitly confirmed for metal clusters by X_{α} –SW calculations in the Ni–Pd–Pt column (R. P. Messmer, S. K. Knudson, K. H. Johnson, J. B. Diamond, and C. Y. Yang, *Phys. Rev. B*, **13**, 1396 (1976); R. P. Messmer, D. R. Salahub, K. H. Johnson, and C. Y. Yang, *Chem. Phys. Lett.*, **51**, 84 (1977).
 (53) F. A. Cotton and E. Pedersen, *Inorg. Chem.*, **14**, 388 (1975).
 (54) Others have independently arrived at this same conclusion using the energy-level diagrams for $Mo_2Cl_8^{4-}$ and $Mo_2(O_2CH)_4$ and the results of resonance-Raman experiments on $[Ru_2(O_2CR)_4]Cl$ (R. J. H. Clark and M. L. Franks, *J. Chem. Soc., Dalton Trans.*, 1825 (1976)).
 (55) J. G. Norman, Jr. and G. E. Renzoni, in preparation.

.h

Crystal and Molecular Structure of a Covalent Perchloric Acid Ester: *p*-Tolylsulfonylmethyl Perchlorate

Jan B. F. N. Engberts,* Hans Morssink, and Aafje Vos*

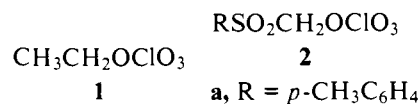
Contribution from the Department of Organic Chemistry and Department of Structural Chemistry, The University, Zernikelaan, Groningen, The Netherlands. Received June 9, 1977

Abstract: The crystal and molecular structure of *p*-tolylsulfonylmethyl perchlorate (**2a**) has been analyzed by x-ray diffraction methods. The crystals are monoclinic, the space group is $P2_1/c$; $a = 11.796$ (3), $b = 5.242$ (2), $c = 20.320$ (5) Å, $\beta = 114.28$ (2)°. The structure has been refined to an R factor of 0.072 on 1723 reflections with $|F_o| > 3\sigma_c(F_o)$. The bond lengths and angles around the central methylene carbon (C(8)) unequivocally demonstrate the covalent bonding between C(8) and O(3) of the perchlorate group. Important molecular parameters are as follows: C(8)–S(1) = 1.805 (4), C(8)–O(3) = 1.423 (5), Cl(1)–O(3) = 1.641 (4), Cl(1)–O(4) = 1.397 (5), Cl(1)–O(5) = 1.379 (5), and Cl(1)–O(6) = 1.407 (6) Å. The reduced π character of the Cl(1)–O(3) bond is reflected in the marked increase in bond length relative to the other Cl(1)–O bonds. Short intermolecular C–H...O distances (H(82)...O(2) = 2.184 (3) Å) indicate strong intermolecular hydrogen bonding between the methylene protons and a sulfonyl oxygen atom of an adjacent molecule.

Ever since the preparation of ethyl perchlorate (**1**) by Hare and Boye¹ in 1841, it has been recognized that most neat perchlorate esters, in which the ClO_4 function is covalently bound to carbon, are extremely hazardous compounds, being sensitive to heat, shock, and friction.² Their strong explosive violence has not encouraged structural³ and chemical investigation^{4,5} despite the obvious theoretical interest⁶ and easy synthetic accessibility⁷ of these types of compounds.

Recently, crystalline and relatively stable alkyl- and aryl-

sulfonylmethyl perchlorates (**2**) were prepared from the reaction of α -diazosulfones with perchloric acid.⁸



Employing appropriate safety precautions, handling of small (ca. 0.1 g) quantities of these compounds involves little hazard